Gulf Stream Meander Propagation Past Cape Hatteras

DANA K. SAVIDGE*

Center for Coastal Physical Oceanography, Old Dominion University, Norfolk, Virginia

(Manuscript received 31 July 2003, in final form 30 March 2004)

ABSTRACT

The propagation and growth characteristics of Gulf Stream meanders past the stream's separation point at Cape Hatteras are analyzed using yearlong time series from a mooring program sponsored by the Minerals Management Service, which included moorings imbedded in the Gulf Stream cyclonic flank both upstream (south) and downstream (north) of Cape Hatteras. In the upstream region, energetic meanders of 3–8-day period, 180–380-km wavelength propagate downstream along the Gulf Stream at speeds of 40–55 km day^{-1}. This variability decays almost completely across the Gulf Stream separation, with growth in lower-frequency variability (30–120 day) in the downstream direction. Wavelength and phase speed in the 3–8-day band are strong functions of frequency, with increasing phase speed for increasing wavenumber. Phase speeds upstream from Cape Hatteras and across the Gulf Stream separation point are faster for a given wavenumber than downstream from Cape Hatteras, in keeping with prior published estimates. At the upstream end of the study site, both baroclinic and barotropic mechanisms contribute to the decay of 3–8-day meanders and growth of lower-frequency 30–120-day variability in the downstream direction. At the downstream end of the study region, the reverse holds, with both baroclinic and barotropic mechanisms contributing to growth of 3–8-day meanders and decay of lower-frequency 30–120-day variability.

1. Introduction and background

The propagation and growth characteristics of Gulf Stream meanders have been extensively studied both upstream (Webster 1961; Brooks and Bane 1981, 1983; Bane et al. 1981; Glenn and Ebbesmeyer 1994a) and downstream (Watts and Johns 1982; Tracey and Watts 1986) from Cape Hatteras. The mean Gulf Stream path follows the shelf edge closely upstream from (south of) Cape Hatteras so that meanders are constrained in amplitude and growth by the large potential vorticity gradient associated with the depth gradient across the continental slope. Between the Charleston Bump (a local topographic high characterized by divergence of the 200–600-m isobaths at about 31°N) and Cape Hatteras (at about 35.5°N), meander amplitudes first experience dramatic growth, then decay from an approximately 50 km maximum to 10 km or less (Miller 1994). On the basis of one-to-several-month current time series, meanders in this upstream region have been characterized as typically 100–250 km in wavelength, with periods of 7–8 days, and propagation speeds near 30–40 km day^{-1} (Brooks and Bane 1981). Both barotropic and baroclinic energy conversion processes have been implicated in the rapid growth in meander amplitudes immediately downstream (north) of the Charleston Bump (Dewar and Bane 1985; Luther and Bane 1985) and in the gradual decay of the meanders from there northward to Cape Hatteras (Lee et al. 1991). Cold-core eddies shoreward of the Gulf Stream are associated with seaward meander displacements (troughs). The effect of these cold-core eddies and their associated vertical velocities has been studied in detail in the South Atlantic Bight (SAB) (see, e.g., Atkinson et al. 1985).

Downstream from Cape Hatteras, in the region from approximately 73° to 68°W, Gulf Stream meanders increase in amplitude from ~10 to ~100 km, except for a local minimum in meander amplitude at 70°W (Lee and Cornillon 1996a). Tracey and Watts (1986) have used 36-month-long records of Gulf Stream position from inverted echo sounders (IESs) to characterize meanders in this region. Here the most energetic meanders are 180–460 km in wavelength, with periods of 4–100 days, and propagation speeds ranging from 45 to 15 km day^{-1}. Meander variance doubles downstream every 50 km, from about 20 km at 73°W to 95 km at 71.5°W (Tracey and Watts 1986). Meanders downstream from Cape Hatteras have slightly slower phase speeds for given wavenumbers than meanders upstream from the cape (Bane et al. 1981; Brooks and Bane 1981; Tracey and Watts 1986). Downstream from Cape Hatteras, the

* Current affiliation: Skidaway Institute of Oceanography, Savannah, Georgia.

Corresponding author address: Dana K. Savidge, Skidaway Institute of Oceanography, 10 Ocean Science Circle, Savannah, GA 31411.
E-mail: dsavidge@skio.peachnet.edu

Gulf Stream has separated from the continental shelf and flows over the continental rise. Water depth increases from 2000 to 4500 m downstream, and the slope of the underlying bathymetry decreases from 0.005 to 0.001 (Sutyrin et al. 2001). Meanders in this region appear to derive their energy from the mean stream through baroclinic instability (Dewar and Bane 1989b), but the effectiveness of that mechanism is constrained by the bottom slope such that meanders do not grow without bound in this region (Sutyrin et al. 2001). Farther downstream, near 68°W, the bathymetric slope is even smaller, and Gulf Stream variability is characterized by the growth of very steep quasi-stationary meanders through baroclinic instability (Watts et al. 1995; Lindstrom and Watts 1994; Cronin and Watts 1996; Cronin 1996; Lindstrom et al. 1997; Savidge and Bane 1999a,b; Howden and Watts 1999; Howden 2000). These very steep meanders can pinch off and become warm- or cold-core Gulf Stream rings, a process that does not occur westward of this location (Lee and Cornillon 1996a). This process will not be discussed in the present work.

Observational programs near Cape Hatteras have tended to focus either north or south of this biogeophysical boundary, with few mooring arrays or hydrographic survey efforts encompassing both regimes. Satellite imagery is difficult to use for meander tracking near Cape Hatteras because of the small meander amplitude there, relative to Advanced Very High Resolution Radiometer (AVHRR) SST horizontal resolution, recurrent cloud cover, and the prevalence of stranded Gulf Stream water overwashing the narrow shelf. Regional-scale computer modeling is particularly difficult here, with large along-shelf variability in physical boundaries, density structure, and boundary forcing, an energetic boundary current impinging on a narrow shelf and separating, large along-shelf convergence on the shelf itself, energetic meteorological forcing, and large seasonal variability.

As a result, the nature of meander propagation past the Gulf Stream separation point near Cape Hatteras has been studied very little. The decay of meanders from the Charleston Bump to Cape Hatteras, combined with the net import of new nutrients to the North Carolina shelf from the stranding of cold upwelled water in meander-associated cold eddies has led Lee et al. (1991) to suggest that these cold-core eddies may not propagate past Cape Hatteras. An appropriate further question is whether the meanders themselves, which have decayed to quite low amplitude here, progress past Cape Hatteras either. The slope becomes quite steep and narrow at Cape Hatteras, downstream from which the Gulf Stream separates from the continental shelf and enters a region with much gentler bottom slope. The effectiveness of baroclinic instability mechanisms in generating meander variability along the Gulf Stream depends critically on cross-stream potential vorticity gradients, and these in turn depend critically on cross-stream gradients in bottom depth (Pedlosky 1987; Johns 1988). It would not be inconceivable that meanders might not survive this abrupt transition at Cape Hatteras. On the other hand, it is reasonable to expect upstream variability to have some effect on variability downstream (Vazquez and Watts 1985; Cronin et al. 1992). Glenn and Ebbesmeyer (1994b) tracked two floats seeded into a cold eddy upstream from Cape Hatteras past the cape. Their success in fitting a propagating ellipse model to the float tracks both upstream and downstream from Cape Hatteras suggested that the floats' propagation was due to the propagation of the intact eddy itself, and presumably the meander it was associated with, past Cape Hatteras.

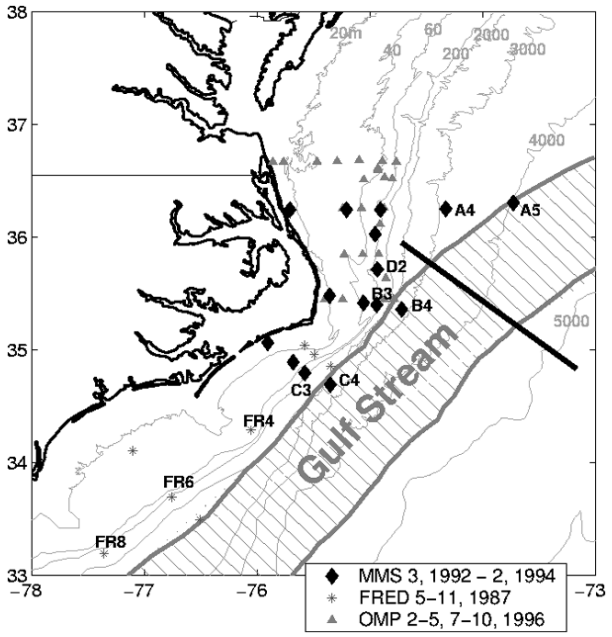

FIG. 1. Cape Hatteras field study site (Mar 1992–Feb 1994), with mooring locations (black diamonds) along three cross-shelf lines (lines A, B, and C, from north to south) and one shelf-edge line (line D) shown. For reference, mooring locations for the Frontal Eddy Dynamics experiment (FRED: gray asterisks) and the Ocean Margins Project (OMP: gray triangles) are also shown. Mooring locations for time series used in this study are labeled with their mooring names (A5, A4, B3, B4, etc.). A schematic Gulf Stream is shown. The black bar across the Gulf Stream midway between moorings B4 and A5 is the location of the CTD section utilized herein.

One valuable addition to the database near Cape Hatteras comes from a 2-yr-long mooring array funded by the Minerals Management Service (Berger et al. 1995). Fifteen mooring locations along three cross-shelf lines bracketing Cape Hatteras were maintained for two years (Figs. 1 and 2). The seawardmost moorings on each of these lines were on the 2000- or 3000-m isobath, imbedded in the Gulf Stream at locations situated both upstream and downstream from the Gulf Stream separation from the continental shelf. The study site is upstream (southwest) from the region studied by Tracey and Watts (1986) and Watts and Johns (1982). In the following, Gulf Stream meander characteristics will be

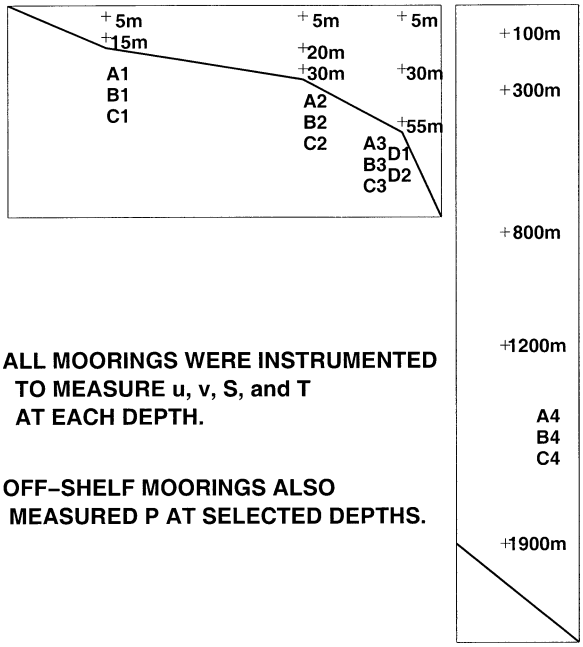

FIG. 2. Schematic mooring line design. Shelf moorings were situated at the 20-, 35-, and 60-m isobaths, with slope moorings at the 2000- and 3000-m isobaths. Mooring numbers increment from 1 to 4 or 5 in the seaward direction. (left) Shelf and shelf-edge moorings had two–three instrument packages in the vertical direction, including InterOcean S4 and General Oceanic MkII winged current meters (*u*, *v*), with temperature (*T*) and salinity (*S*) sensors. (right) Slope moorings had five (A4, B4, C4) or six (A5, not shown) instrument packages in the vertical, including General Oceanic MkI/MkII winged current meters and Aanderaa RCM 7/8s, with *T*, *S*, and pressure (*P*) sensors.

assessed from these data. Meander characteristics upstream from Cape Hatteras will be defined over a broader frequency range than has been possible before. Phase speeds upstream from Cape Hatteras are shown to be faster than meanders downstream from Cape Hatteras over a broad wavenumber band. Cross-spectral analysis indicates that Gulf Stream 3–8-day meanders do not propagate past Cape Hatteras. Lower-frequency variability increases in the downstream direction. Both baroclinic and barotropic instability mechanisms are implicated.

2. Data

The data used in this study were collected by a multi-institutional team funded by the Minerals Management Service (Berger et al. 1995). Fifteen mooring locations across and along the Cape Hatteras shelf and slope were maintained from March 1992 through February 1994 (Figs. 1 and 2). These moorings were situated along three cross-shelf lines bracketing Cape Hatteras and one along-shelf line at the shelf edge. Preliminary findings were summarized in a technical report at the conclusion of the field project (Berger et al. 1995).

Shelf moorings at the 20-, 35-, and 60-m isobaths were instrumented with InterOcean S4 and General Oceanic MkII winged current meters, which also measured salinity (*S*) and temperature (*T*). Slope moorings on the 2000- and 3000-m isobaths had five–six instrument packages in the vertical direction, utilizing Aanderaa current meters to measure temperature, salinity, and pressure (*P*), along with current speed (*V*) and direction. Raw data were first 3-h low-pass (3-HLP) filtered with a Lanczos kernel (subsampled hourly), then 48-HLP (Hanning) filtered (subsampled daily). Both hourly and daily data are used in the following.

Pressure and velocity data from the uppermost instrument packages are shown for the slope moorings A5, B4, and C4 for the first year of the 2-yr mooring deployment (Fig. 3). It is apparent from the vector plots that these moorings were imbedded in the Gulf Stream until the early part of January 1993. To monitor meanders at the mooring locations, some measure of the Gulf Stream's position relative to the mooring locations is necessary. Of the variables measured by the upper instrument packages at moorings A5, B4, and C4, pressure proves to be most useful for this purpose. If the mooring line were rigid, each current meter and *T* sensor would stay at the same depth in the water throughout the deployment, and measured *T* and *V* would increase as the shoreward half of the Gulf Stream jet moved closer to the shelf edge across a particular mooring location (Fig. 4). However, since the mooring is not rigid, as the Gulf Stream jet shifts toward the shelf edge, the mooring line is pulled down in the water column by the integrated drag of the large Gulf Stream currents (Hogg 1986, 1991). Since *T* and *V* fall off with depth in the Gulf Stream, this effect will compete with the expected increase in *T* and *V* as the Gulf Stream axis moves shoreward and tilts the mooring. This confounds the usefulness of either *T* or *V* at a given mooring as an indicator of where in the stream the mooring is. However, pressure was also measured at these upper instrument packages. As the mooring line is pulled down in the water column with Gulf Stream shoreward shifts, the pressure records indicate how far in the vertical the particular mooring has been dragged down, varying monotonically with the integrated current velocity impinging on the mooring line. Note the large amplitude of the pressure variability, in excess of 200 dbar (Fig. 3). Savidge and Bane (2001) demonstrated through cross-spectral analysis that the upper-level pressure record at mooring B4 was highly coherent with surface-intensified Gulf Stream velocities over a broad frequency range, with low coherence with subthermocline velocities on the same mooring line. Similar findings apply at A5 and C4, illustrated here in a simplified way through zero-lag correlation coefficients (Table 1), which show correlations decreasing with depth between velocity magnitudes and upper-level pressure fluctuations at all three locations. One caveat for the 6–7-day band is that, at A5, Gulf Stream variability in that band has fallen to such low levels that middepth velocity magnitudes are more correlated with the upper-level

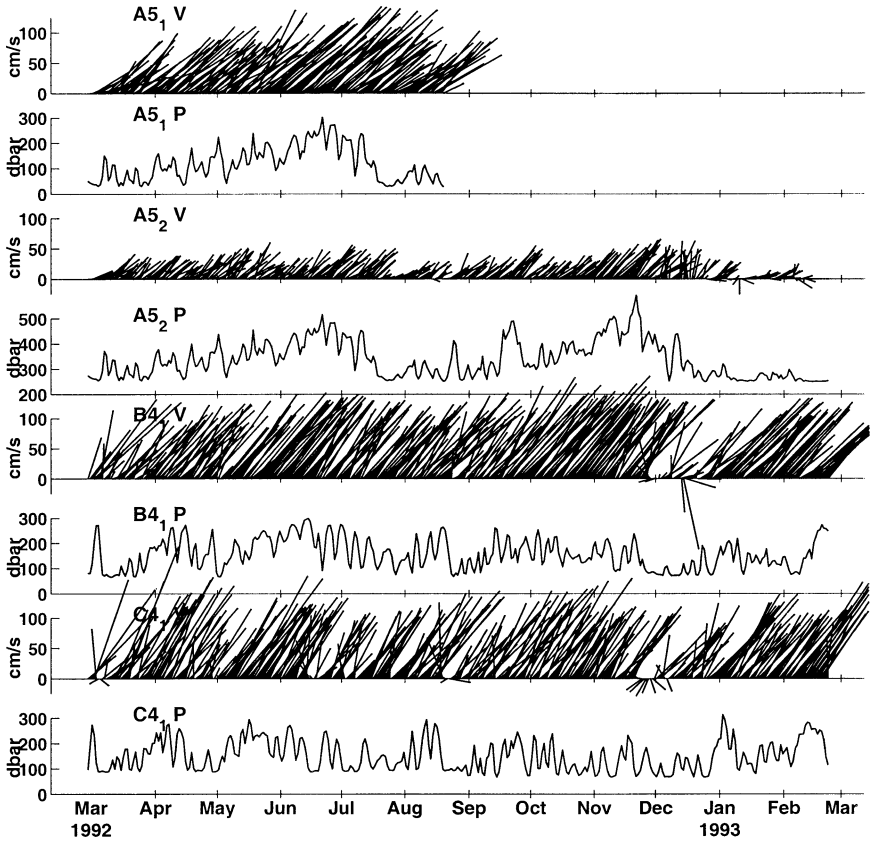

FIG. 3. Selected time series from the Gulf Stream imbedded moorings. Stick plots represent velocities from nominal depths of (top) 100 m at mooring A5, (third from top) 300 m at mooring A5, (fifth from top) 100 m at mooring B4, and (seventh from top) 100 m at mooring A5. Vertical sticks represent northward velocities. The remaining time series are pressure records from (second from top) 100 m at mooring A5, (fourth from top) 300 m at mooring A5, (sixth from top) 100 m at mooring B4, and (bottom) 100 m at mooring A5.

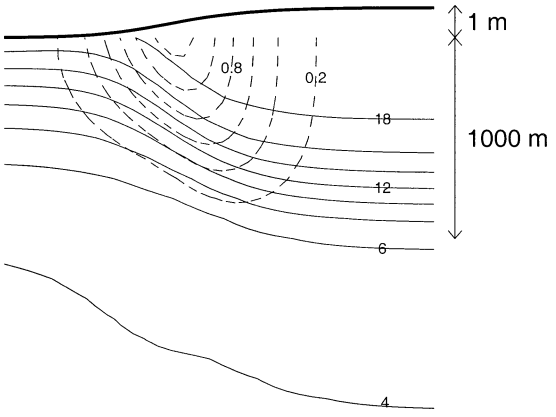

FIG. 4. A schematic Gulf Stream, calculated from the Hall (1994) synthetic *T* section using the *T–S* relationship for the North Atlantic of Armi and Bray (1982). Velocities were referenced to 1215-m depth, as described in the text. Sea surface height was calculated from dynamic height calculations.

pressure records, despite low magnitudes of currents and pressure fluctuations at that periodicity, relative to the other moorings. At all three mooring locations, it is possible that upper-level southwestward currents shoreward of the Gulf Stream front (associated with Gulf Stream filaments) may also appear in the record, making it less useful as a representation of Gulf Stream distance offshore. Visual inspection of the time series indicates pressure fluctuations coincide with strong upper-level northeastward flow, not with southwestward Gulf Stream filament-associated currents, which are relatively uncommon in these datasets.

One further consideration is that Gulf Stream velocities do not increase monotonically across the stream, but (disregarding Gulf Stream filaments) increase from the shoreward edge seaward to a maximum at the Gulf Stream axis (the cyclonic flank) and decrease seaward of the maximum (the anticyclonic flank; Fig. 4). In the anticyclonic flank, shoreward shifts in Gulf Stream position would be associated with decreases in vertically integrated velocity and lower pressure values, opposite to the relationship in the cyclonic flank. In order to

TABLE 1. Zero-lag correlation coefficients between first-year hourly upper-level pressures and velocity magnitudes at each depth on the moorings. Numbers of samples are in parentheses.

	A5 $P_{300\ m}$	B4 $P_{100\ m}$	C4 $P_{100\ m}$
$V_{100\ m}$	0.83 (4209)	0.77 (7437)	0.73 (6332)
$V_{300\ m}$	0.69 (7436)	0.69 (7437)	No data
$V_{800\ m}$	0.43 (7436)	0.24 (7437)	0.24 (6332)
$V_{1200\ m}$	0.38 (7436)	0.20 (7437)	0.18 (6330)
$V_{1900\ m}$	0.10 (7436)	0.25 (7437)	0.08 (6331)
$V_{2900\ m}$	0.15 (7436)	No data	No data

accept that pressure represents Gulf Stream meander variability, it is therefore necessary to demonstrate that the moorings were imbedded in the cyclonic flank of the Gulf Stream throughout the record and did not cross seaward of the Gulf Stream axis into the anticyclonic flank.

The characteristic temperature cross-section associated with the Gulf Stream jet structure (through thermal wind) allows such a demonstration to be made. Since isotherms descend monotonically across both the cyclonic and anticyclonic flanks of the (mean) Gulf Stream (Fig. 4), the cyclonic flank is consistently warmer than the anticyclonic side at similar depths. Here, mooring A5 data have been plotted in temperature–pressure (*T–P*) space and compared with two separate representations of ''typical'' Gulf Stream structure in *T–P* space (Fig. 5). The first is a 1990 CTD section across the Gulf Stream (Savidge et al. 1993) at a location approximately midway between the Cape Hatteras mooring (B4) and the downstream mooring (A5) (Fig. 1). The second Gulf Stream representation is the ''synthetic'' Gulf Stream at 65°W of Hall (1994) (from XBT data). Temperature–pressure data from these sections were interpolated and plotted for 10-dbar vertical spacing and near 10-km horizontal spacing. After calculating salinity from temperature for the Hall (1994) synthetic section [using the *T–S* relationship for the North Atlantic of Armi and Bray (1982)], velocity fields were calculated from the CTD- and XBT-based density fields using the dynamic method (referenced to 1215 m) and used to specify the cyclonic or anticyclonic flanks for the sections. From the comparison between mooring data from the 300-m depth instrument package at mooring A5 and the two Gulf Stream sections, it is clear that the mooring did not sample the Gulf Stream anticyclonic flank. Moorings B4 and C4 show equivalent results.

An additional aspect of the pressure variability is of interest. While high coherence between the 100- and 300-m velocities is noticable (Fig. 3), the two time series actually record relatively independent information, representing vertical variability in the measured velocities. The fact that they are well correlated (Berger et al. 1995) illustrates vertical coherence in Gulf Stream structure. The pressure time series at 100- and 300-m depth are not independent records—each depends on the integrated velocity impinging on the mooring line below the instrument. In fact, coherence between the pressure records at 100- and 300-m depths at mooring A5 exceeds 0.99 over essentially all subtidal frequencies (not shown). Use of the 300-m record at mooring A5 allows Gulf Stream variability to be characterized over a longer

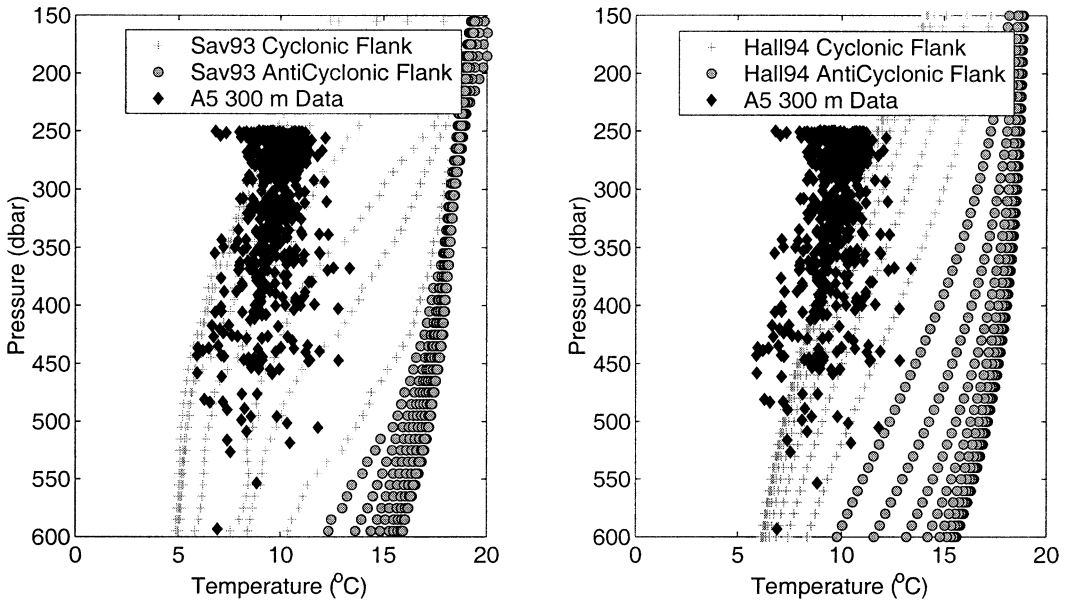

FIG. 5. Temperature–pressure plots comparing two sample Gulf Stream sections with data from mooring A5 overplotted. Temperatures and pressures from the cyclonic (plus signs) and anticyclonic (gray circles) flanks of the Gulf Stream, determined as described in the text, are shown. (left) Gulf Stream section data from a 1990 CTD section taken a short distance downstream from Cape Hatteras (location is marked in Fig. 1). (right) The Gulf Stream representation is the ''synthetic'' Gulf Stream at 65°W of Hall (1994).

time frame than is possible with the shorter 100-m record (172 days). The Gulf Stream moved southward of mooring A5 during the early part of 1993 and remained southward for nearly 6 months. In this paper, data from before January 1993 will be used: times when the 300-m pressure instrument at A5 was functioning, and before the Gulf Stream moved southward of the A5 mooring. This yields a 308-day time series for analysis.

3. Meander spectral analysis

In the following, Gulf Stream position proxies (the upper-level pressure records at moorings A5, B4, and C4) will be used to assess meander and meander propagation characteristics immediately upstream and downstream from the Gulf Stream separation at Cape Hatteras. These spectral and cross-spectral analyses used the multitaper method in order to obtain the most information possible about long-period fluctuations. The more typically used Welch's overlapped segment averaging (WOSA) method reduces variance by dividing each time series into overlapping segments, tapering each segment with an identical filter to reduce bias, running the spectral analysis on each segment, and then averaging the results over all segments by frequency (Percival and Walden 1993). This reduces the information available at long periods. The multitaper method uses a series of different tapers on the complete time series to reduce bias, with spectral analysis on each differently tapered version of the data, averaged over all realizations to reduce variance (Percival and Walden 1993). Without any series length reduction, more information is preserved about the longer-period variability. Using successively more tapers reduces variance of the final averaged spectral estimate but introduces increasing bias in the spectral estimates. If the investigator is content with high bandwidth (poor frequency resolution), it is possible to get very high reduction of variance with very little introduction of bias. For the present case a duration times half-bandwidth product of 6 was chosen, allowing for a total of 11 discrete prolate spheroidal sequences to be used as tapers. The resulting variance is quite low, as are the 90% and 95% confidence threshold levels for coherence. Prior to the spectral and cross-spectral analyses, the pressures were detrended, and all time series were demeaned and normalized by their standard deviations. Hourly 3HLP data are used, in order to assess phase lags simply and well. Analyses using 48HLP data show equivalent results.

a. Gulf Stream separation point

First it is necessary to confirm that the Gulf Stream separates from the continental shelf between moorings B4 and A5, as satellite imagery suggests (not shown). Coherence is significant between the Gulf Stream position proxy at B4 and velocity magnitude in the midwater column at the 60-m isobath shelfbreak mooring (B3) on the B line (21-km separation; Fig. 6). Conversely, coherence is low between the Gulf Stream position proxy at B4 and velocity magnitude at D2, the 60-m isobath shelfbreak mooring 35 km north of mooring B3. The larger distance between moorings B4 and D2 (44 km) does not account for the lower coherence since the Gulf Stream position proxy at mooring C4 along the C line is nearly as coherent with velocity magnitude at B3 (87-km separation) as the Gulf Stream position proxy at mooring B4 is. Instead, the low coherence between the Gulf Stream variability at B4 and velocities at D2 illustrate that the stream has separated from the shelf by the D2 shelf-edge location, and so does not dominate the variability there, as it does at B3.

b. Along-stream pairwise spectral analysis

Variance-preserving spectra of the Gulf Stream position proxies from the slope moorings upstream from the Gulf Stream separation (C4 and B4) show high energy over the 3.8–8.7-day-period band, with highest values centered broadly about 4.65 and 6.7 days (Fig. 7a). The energy downstream from the Gulf Stream separation at mooring A5 is much lower at those periods. The lower energy in the A5 spectrum is not due to use of data from the deeper 300-m instrument since the A5 100- and 300-m pressure spectra for the shorter period of the 100-m data show equivalent values at these periods (not shown). Gulf Stream variability at A5 exhibits higher energy at long periods than the upstream moorings at 45-day periods and longer.

The cross-spectrum between the mooring pair upstream from Cape Hatteras, C4 and B4, shows high coherence over a broad range of frequencies, including the 3.8–8.6-day meander band where energies in the variance-preserving spectra for C4 and B4 were highest (Figs. 7a,b). Phase lags are a strong function of frequency and indicate downstream propagation of meanders in this band (Fig. 7c). Coherence between moorings B4 and A5, bracketing the Gulf Stream separation point, is weak at best, exceeding the 95% confidence level over very limited ranges at 2.5–2.6 days and 4.5–5.5 days. The peak at 8 days represents a relatively low energy band in Gulf Stream variability at the downstream mooring, A5.

The contrast of high coherence between the upstream mooring pair with the low coherence between the downstream mooring pair suggests that meander propagation characteristics may undergo some fundamental change as they encounter the Gulf Stream separation point at Cape Hatteras. It seems unlikely that the coherence difference represents simply decreasing coherence with increasing distance along-stream given the very large differences in coherence between two regimes, the relatively modest increase in downstream distance between the downstream pair (50%), and the fact that meander wavelengths exceed the downstream separation. Upstream from Cape Hatteras, along-shelf coherences from

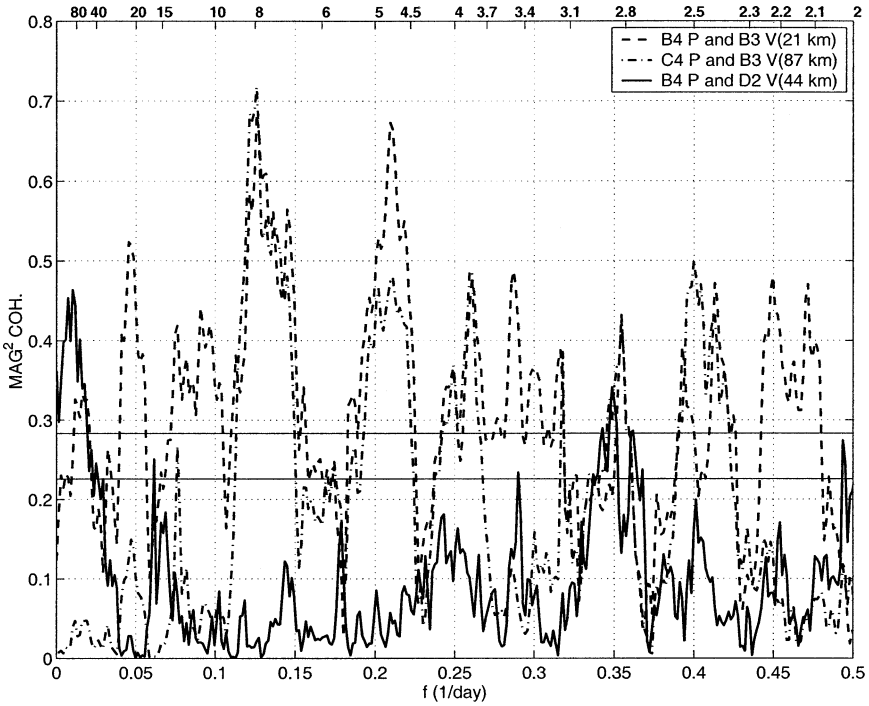

FIG. 6. Cross-spectra between shelf-edge velocity magnitudes at B3 and D2 and the Gulf Stream position proxies at B4 and C4. Horizontal lines are the 90% and 95% significance levels. Horizontal separation between each pair of moorings is shown in the figure legend.

the 6-month Frontal Eddy Dynamics experiment (FRED) moorings suggest coherences over the 2–10-day-period meander band at up to 171-km along-shelf separation (not shown). Downstream from Cape Hatteras, Tracey and Watts (1986) found coherence at the 90% confidence level in the meander band at separations of up to 191 km in the downstream direction. Their correlations do not fall off as abruptly with increasing distance along-stream as the MMS data do. Apparently the poor correlation across the Gulf Stream separation in the MMS data is not due to intrinsically short Gulf Stream meander decorrelation scales.

c. Propagation characteristics

Meander propagation characteristics can be calculated from cross-spectral phase and coherence values for frequency bands where peaks exist in the spectra, and the coherence along-stream exceeds the 90% confidence threshold. An effort has been made to select frequency bands with width approaching the resolution half-bandwidth of the cross-spectral estimates and range from 0.05 to 0.1 day^{-1} width in frequency. For these frequency bands, average phase speed (C_p), wavelength (Λ), and wavenumber (K) have been calculated as

$$C_p = Yf \Big/ \frac{\phi}{2\pi}$$

(Watts and Johns 1982), $\Lambda = C_pT = C_p/f$ and $K = 2\pi/\Lambda$ (Pond and Pickard 1983); Y is the along-shelf separation between moorings, ϕ is the phase lag, f is the frequency, and $T = 1/f$ is wave period. Values have been calculated for each frequency and then averaged over the frequency band of interest. The resulting values are strong functions of frequency, with phase speeds of 40–55 km day^{-1} and wavelengths of 180–380 km over the meander band (Fig. 8).

The dispersion diagram indicates increasing phase speed with wavenumber (Fig. 9), in keeping with previous estimates by Tracey and Watts (1986) for the region just downstream from mooring A5. Note also that the phase speeds are consistently higher for a given wavenumber than those found by Tracey and Watts (1986). This is also in keeping with their suggestion that phase speeds may decline downstream from Cape Hatteras and with the phase speeds found by Brooks and Bane (1981) for limited frequency bands off Onslow Bay (the second shallow embayment along the Carolina coast south of Cape Hatteras). To the extent that meanders propagate across the separation zone, their speeds are more consistent with propagation speeds found upstream from Cape Hatteras.

4. Energetics

Berger et al. (1995) suggest evidence for baroclinic instability of relevance to the along-stream changes in meander frequency characteristics seen in section 3b.

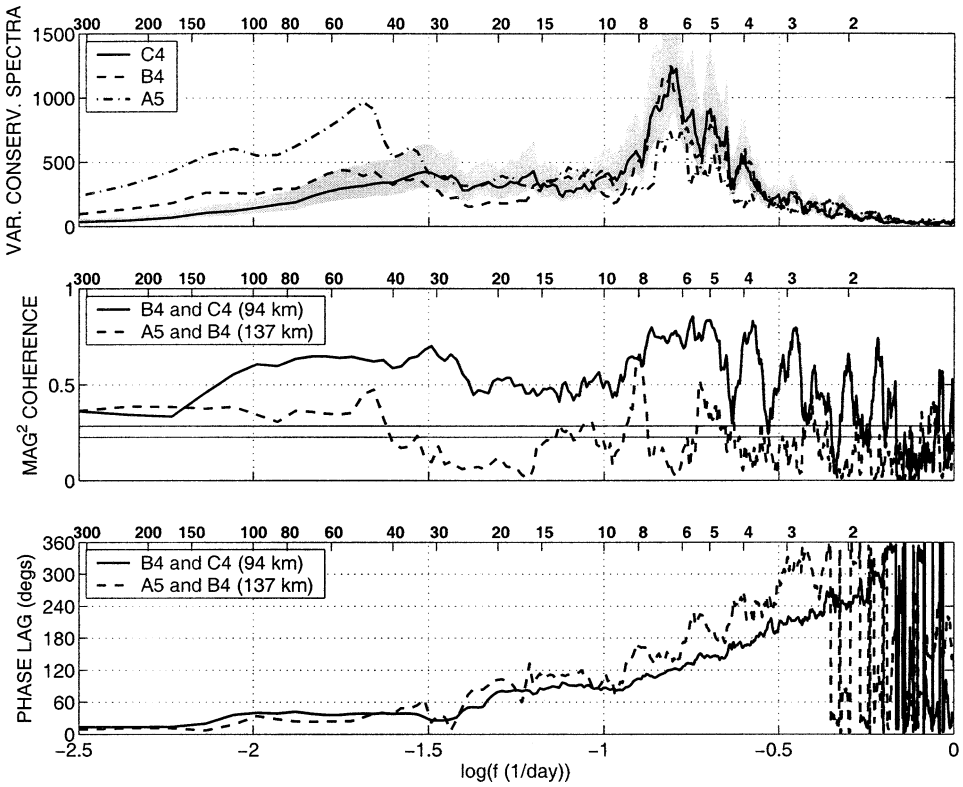

FIG. 7. (top) Variance-preserving spectra, (middle) cross spectra, and (bottom) phase lags between the Gulf Stream position proxies at A5, B4, and C4 (308-day pressure records). Horizontal lines in the cross-spectral plot are the 90% and 95% significance levels. Horizontal separations between mooring pairs are indicated in the legends. The 90% confidence envelope in the variance-preserving spectral plot (top panel) was calculated using a χ^2 distribution for 20 equivalent degrees of freedom, estimated according to Percival and Walden (1993, p. 370).

Using complex empirical orthogonal function analysis (CEOF) of currents above and below the thermocline at B4 for variability in frequency bands of 4–11, 13–27, and 27–345 days, they defined a first mode that accounted for a significant fraction of the total variability from all depths in these bands. The phase lags between subthermocline and upper-layer variability in the first mode were consistent with growth in the 27–345-day band and decay of the 4–11-day band through baroclinic instability processes (see Berger et al. 1995; their section 3.3 and Fig. 3.3-2). Spectral analyses from the present study designed to address this issue provide little support for the CEOF findings of Berger et al. (1995) (not shown). Coherences at moorings A5, B4, and C4 between lower-layer measures (velocity magnitudes or components) and upper-level measures (pressures or velocity magnitudes or components) were, in general, poor. One exception was a marginally significant band at B4 between lower-layer along-shelf velocity and upper-layer pressure at periods from 15 to 150 days. The phase lag associated with this broad band was in the same sense that the CEOF analysis indicated and is consistent with eddy growth through baroclinic instability. However, the primary result from spectral analyses is no result. To the extent that meander variability is not periodic, it may be that CEOF analysis is more suited to this task.

Another approach to assessing the importance of baroclinic and barotropic instability processes near Cape Hatteras is to use data from a particular level to calculate energy conversion terms from eddy covariances and mean gradients. As summarized in Lee et al. (1991), and references therein, these terms are

$$\overline{u'v'}\frac{\partial \overline{v}}{\partial x} \quad \text{(barotropic)} \quad \text{and}$$

$$\frac{g}{\overline{\rho}}\overline{u'\rho'}\frac{\partial \overline{\rho}}{\partial x}\left|\frac{\partial \overline{\rho}}{\partial z}\right|^{-1} \quad \text{(baroclinic).}$$

For convenience and clarity, the absolute value of $\partial\overline{\rho}/\partial z$ converts the negative isopycnal slopes of the cyclonic flank of the Gulf Stream to positive values. With this convention, negative-valued energy conversion terms signify barotropic or baroclinic growth of eddy variability, while positive values express decay of variability feeding the mean kinetic or potential energy.

These terms have been evaluated for the frequency

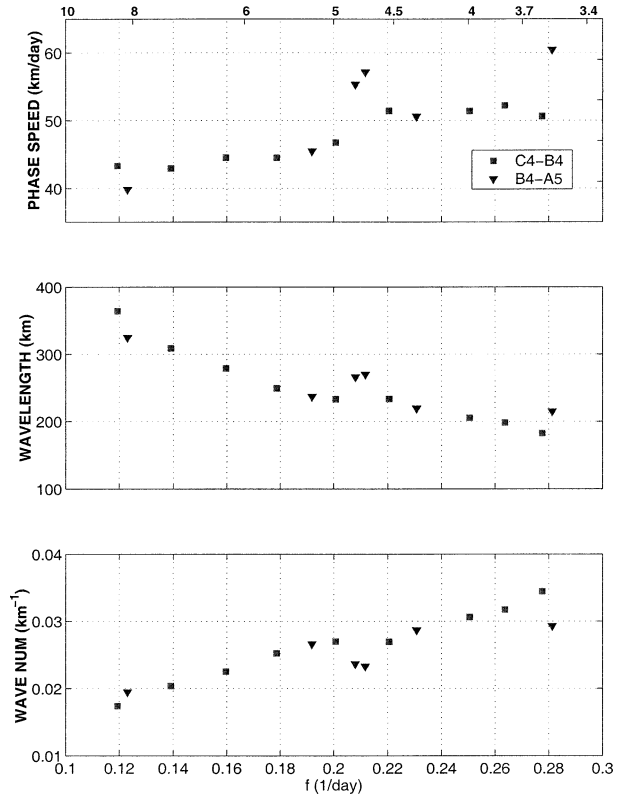

FIG. 8. Propagation characteristics as a function of frequency. (top) Phase speed and (bottom) wavenumber are increasing functions of frequency; (middle) wavelength decreases with increasing frequency.

bands of interest by constructing 15-day low-passed and 15-day high-passed time series from the 48 HLP data and calculating the energy conversion terms for each. Density and velocity fields from the analytic Gulf Stream temperature section of Hall (1994) (calculated as described in section 2) were used to calculate representative density and velocity gradient values: $\partial\overline{v}/\partial x = 2 \times 10^{-5}\ \mathrm{s}^{-1}$, $\partial\overline{\rho}/\partial x\,|\partial\overline{\rho}/\partial z|^{-1} = -0.008$, $g/\overline{\rho} = 10\ \mathrm{m\ s}^{-2}/1026.8\ \mathrm{kg\ m}^{-3}$. Velocities and temperature at moorings A5, B4, and C4 were interpolated or extrapolated to 300-m depth from the 100- and 300-m instrument packages (which migrated from 100- to 300-m and 300- to 500-m depths because of mooring motion). The along-stream direction was defined by the principal axis of the 300-m interpolated currents at each mooring location. Salinities and densities were then calculated from the 300-m interpolated temperatures, again using the *T*–*S* relationship of Armi and Bray (1982).

From these calculations, baroclinic and barotropic processes appear to be of comparable importance in both the 15–200- and 2–15-day-period bands (Fig. 10, Table 2). Upstream from Cape Hatteras at C4, the signs of both terms indicate eddy decay in the higher-frequency band and growth at lower frequencies. The low-frequency growth appears to be primarily due to baroclinic processes. At the downstream end of the study region at mooring A5, 2–15-day meander growth is apparently reestablished. Baroclinic and barotropic contributions to both the growth of this band, and decay of the low-frequency-band meander variability are evident. The standard errors are large, casting doubt upon the magnitudes and even the signs of these estimates. The major problem with this method has been pointed out by Rossby (1987)—the neglect of energy conversion terms involving along-stream gradients in velocity is unwarranted since they should be of equivalent magnitude to those involving across-stream gradients in velocity. However, estimates of this nature continue in the literature with the implicit assumption that they suggest truth. Here, they are included because of their consistency with the observed along-shelf changes in the calculated Gulf Stream meander spectra and to motivate more legitimate energetics work for the region of Gulf Stream separation in the future. The reported baroclinic and barotropic conversion estimates are consistent with the decay of 2–15-day meanders and the growth of 15–200-day variability in the downstream direction seen in this study with previous expectation and estimates upstream from Cape Hatteras (Lee et al. 1991; Brooks and Bane 1981) and with the previously observed meander growth in the region eastward of this study between Cape Hatteras and the New England Seamount Chain (Lee and Cornillon 1996a,b; Tracey and Watts 1986; Dewar and Bane 1989a,b).

5. Discussion

The long time series at the three MMS moorings imbedded in the Gulf Stream cyclonic flank have afforded the best in situ observations to date of meander propagation along the continental shelf in the meander decay region upstream from Cape Hatteras, and represents the first extensive in situ observations of meander propagation across the Gulf Stream separation from the continental shelf. The primary result herein is that Gulf Stream meanders apparently decay almost completely as they encounter the narrow steep slope near Cape Hatteras and enter the deep ocean. Meander energy clearly decreases downstream such that meander band variability in the 3–8-day band has practically disappeared by mooring A5 (Fig. 7). Clearly the potential vorticity constraints change dramatically along-stream in this region. Nonetheless, it is somewhat unexpected that meanders apparently do not survive the transition. In fact, some meanders clearly do progress past the separation point. For example, a series of four peaks in the pressure records of August 1992 appear in the records from C4, B4, and A5, though the first three peaks are of relatively small magnitude at A5 (Fig. 3). However, these time series also illustrate that identifiable meander propagation past Cape Hatteras is the exception rather than the rule. Conversely, the Gulf Stream position proxies at C4 and B4 are obviously well correlated, with

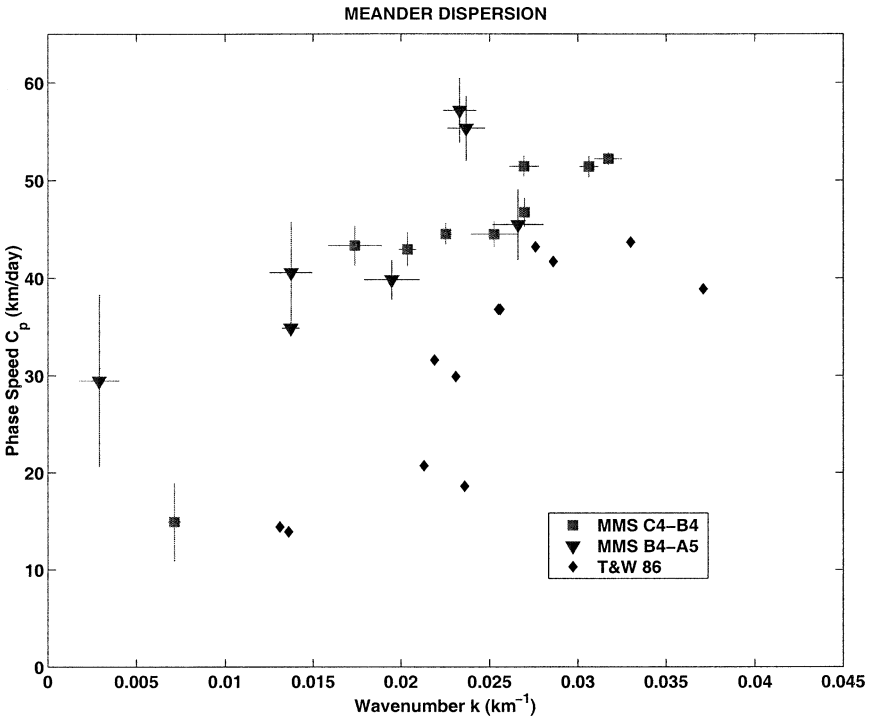

FIG. 9. Dispersion diagram for meander propagation between mooring pairs C4–B4 (squares), and B4–A5 (triangles). Values for meander propagation from the dispersion diagram of Tracey and Watts (1986) are also shown (solid diamonds) for a location slightly farther downstream from Cape Hatteras.

downstream propagation of meanders evident throughout the entire time series.

The issue of background potential vorticity is further complicated by the deep western boundary current (DWBC), which crosses under the Gulf Stream at this location. Moorings A4, B4, and C4 along the 2000-m isobath show southwestward means in 1200-m alongshelf currents (Fig. 11) and so were apparently imbedded in the DWBC. Mooring A5 was not. To the extent that the DWBC constitutes a defined layer of water at the seabed, the overlying layer of water can be stretched or shortened vertically in a given location by variability in the position of the DWBC. Energetic variability in the 20–60-day band dominates these records, likely caused by topographic Rossby waves (TRW). This variability is coherent along the slope, especially between A4 and C4, with southward phase propagation and signal intensification (Fig. 12). DWBC, TRW, and Gulf Stream variability relationships have been investigated in prior datasets from locations just downstream from the MMS field site (Johns and Watts 1986; Dewar and Bane 1989a,b; Pickart and Watts 1990; Pickart and Smethie 1993; Pickart 1994). Those datasets were better suited to the task than the MMS data, because of their cross-stream resolution (MMS arrays had only one mooring in the DWBC or Gulf Stream at any one alongstream location). Dewar and Bane (1989b) suggest that DWBC variability may supply some of the energy necessary for the growth of Gulf Stream meanders in the region immediately downstream from Cape Hatteras. However, the TRW, which would exist even in the absense of the DWBC, effectively mask any intrinsic DWBC variability that might exist over 20–60-day bands and down to the TRW cutoff frequency, ~8 day here (Pickart 1995). Their ubiquity over a broad range of frequencies in which Gulf Stream variability is of interest makes investigation of the Dewar and Bane (1989b) DWBC/Gulf Stream hypothesis difficult to address with datasets of this kind.

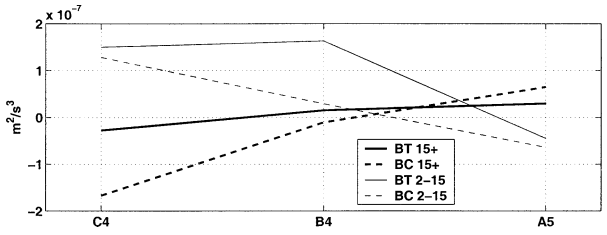

FIG. 10. Baroclinic (dashed lines) and barotropic (solid lines) instability terms. Thick lines represent values for the 15–200-day-period band (denoted ''15+'' in legend); thin lines represent values for the 2–15-day-period band (denoted ''2–15'' in legend). Negative values indicate eddy growth; positive values indicate eddy decay.

Both baroclinic and barotropic processes contribute to the observed along-stream changes in Gulf Stream meander spectral characteristics at this location. This is

TABLE 2. Barotropic (BT) and baroclinic (BC) energy conversion terms for two frequency bands. Positive signs indicate decay of eddy kinetic energy; negative signs indicate growth (see text). Values in parentheses are standard errors. Multiply these values by 10^{-7} m^2 s^{-3}.

Site	2–15 BT	2–15 BC	15+ BT	15+ BC
A5	−0.45 (0.91)	−0.64 (1.90)	0.30 (0.45)	0.65 (0.66)
B4	1.63 (0.28)	0.29 (0.30)	0.15 (0.29)	−0.11 (0.80)
C4	1.50 (0.54)	1.28 (0.81)	−0.28 (0.33)	−1.67 (1.02)

in keeping with previous data-based estimates both upstream and downstream from Cape Hatteras (Bane et al. 1981; Brooks and Bane 1981; Hood and Bane 1983; Dewar and Bane 1985, 1989b; Lee et al. 1991; Tracey and Watts 1986) and with modeling studies in each regime (Luther and Bane 1985; Miller and Lee 1995; Sutyrin et al. 2001). Modeling of the transition between these two vastly different background potential vorticity regimes could help define constraints on Gulf Stream variability in this region and might address the question of Gulf Stream separation from the continental shelf. Modern modeling studies of this process typically focus on longer-term variability in Gulf Stream position and separation point than the MMS dataset allows (Spall 1996a,b; Tansley and Marshall 2000). Yet the observed along-shelf change in spectral characteristics between 3–8- and 30–120-day Gulf Stream variability may be relevant to this as yet poorly understood phenomenon.

Gulf Stream variability is directly relevant to shelf circulation in this region for a variety of reasons. It has long been recognized that Gulf Stream variability is correlated with alongshore current variability on the shelf in the South Atlantic Bight, particularly on the mid- to outer shelf, either through horizontal entrainment or through the imposition of cross-shelf or alongshelf pressure gradients (Atkinson et al. 1985, and references therein). Cross-shelf current variability is also affected since the Gulf Stream position is highly correlated with offshelf export at Cape Hatteras over a broad range of frequency bands (Savidge and Bane 2001). Recently described energetic shoreward currents along the Hatteras front south of Cape Hatteras (the front separating cold fresh Mid-Atlantic Bight (MAB) shelf water from warmer saltier SAB water) may also be modulated by Gulf Stream variability (Savidge 2002).

Regions of meander-band eddy decay have been associated with net nutrient flux onto the continental shelf and net carbon production (Lee et al. 1991). In this region of profound alongshore convergence on the continental shelf (Savidge and Bane 2001), such production may be efficiently exported to the open ocean, depending on the population structure of the consumers of primary production. Ocean Margins Project (OMP) results suggest that most new production in MAB shelf water north of Cape Hatteras may be consumed by small organisms, whose bodies and excretions may not quickly settle out of the water column, instead being exported to the open ocean (Verity et al. 2002a,b). South of Cape

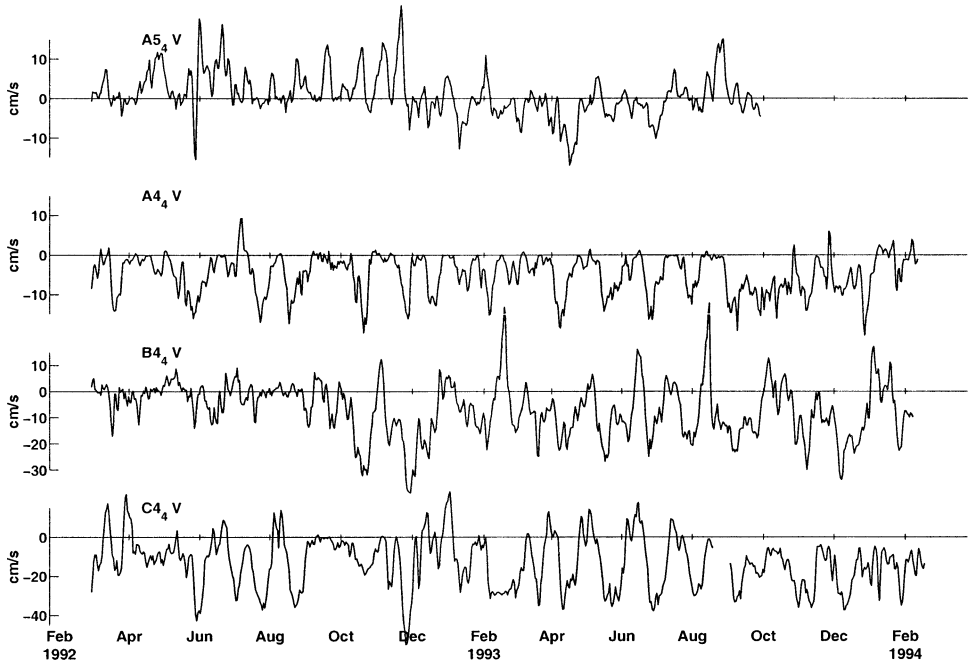

FIG. 11. Along-shelf velocities at 1200-m depth from the slope moorings at A4, A5, B4, and C4. The along-shelf direction was determined from principal axis analysis of the 48 HLP velocities.

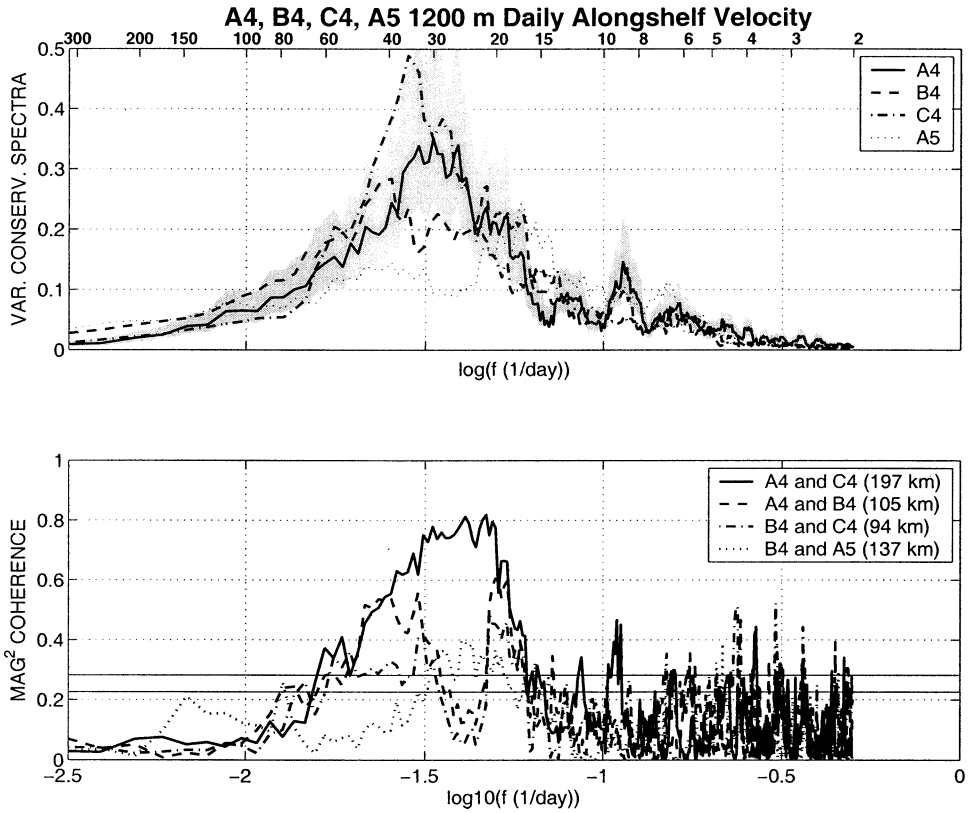

FIG. 12. Variance-preserving spectra and cross spectra between along-shelf 48 HLP velocities at 1200-m depth at the slope moorings at A4, A5, B4, and C4. The along-shelf direction was determined from the principal axis of the velocities. (top) The 90% confidence envelope in the variance-preserving spectral plot was calculated using a χ^2 distribution for 20 equivalent degrees of freedom, estimated according to Percival and Walden (1993, p. 370). (bottom) Horizontal lines in the cross-spectral plot are the 90% and 95% significance levels. Horizontal separation between each pair of moorings is shown in the legend for the bottom panel.

Hatteras, where approximately one-third of the total volume of water exported at Cape Hatteras originates (Savidge and Bane 2001), the population structure of primary consumers may be quite different than in the southern MAB shelf water. [Larval fish populations have been shown to be quite disparate across the Hatteras front (Grothues and Cowen 1999).] If so, the ultimate fate of carbon incorporated into organic tissue south of Cape Hatteras may differ substantially from that originating immediately north of Cape Hatteras. In either case, export of the water in which the organisms are imbedded depends on Gulf Stream variability (Savidge and Bane 2001).

Acknowledgments. Support for this study came from the Center for Coastal Physical Oceanography, Old Dominion University, Norfolk, Virginia. The data were collected for the Minerals Management Service OCS Study MMS 94-0047. Peter Hamilton supplied the FRED data. Remarks from two anonymous reviewers were helpful.

REFERENCES

Armi, L., and N. A. Bray, 1982: A standard analytic curve of potential temperature versus salinity for the western North Atlantic. *J. Phys. Oceanogr.,* **12,** 384–387.

Atkinson, L. P., D. W. Menzel, and K. A. Bush, 1985: *Oceanography of the Southeastern U.S. Continental Shelf.* Coastal and Estuarine Sciences, Vol. 2, Amer. Geophys. Union, 156 pp.

Bane, J. M., D. A. Brooks, and K. R. Lorenson, 1981: Synoptic observations of the three-dimensional structure and propagation of Gulf Stream meanders along the Carolina continental margin. *J. Geophys. Res.,* **86,** 6411–6425.

Berger, T. J., P. Hamilton, R. J. Wayland, J. O. Blanton, W. C. Boicourt, J. H. Churchill, and D. R. Watts, 1995: A physical oceanographic field program offshore North Carolina. Minerals Management Service Tech. Rep., OCS Study MMS 94-0047, U.S. Department of the Interior, New Orleans, LA, 345 pp.

Brooks, D. A., and J. M. Bane, 1981: Gulf Stream fluctuations and meanders over the Onslow Bay upper continental shelf. *J. Phys. Oceanogr.,* **11,** 247–256.

——, and ——, 1983: Gulf Stream meanders off North Carolina during winter and summer, 1979. *J. Geophys. Res.,* **88,** 4633–4650.

Cronin, M., 1996: Eddy-mean flow interaction in the Gulf Stream at 68°W. Part II: Eddy forcing on the time-mean flow. *J. Phys. Oceanogr.,* **26,** 2132–2151.

——, and D. R. Watts, 1996: Eddy–mean flow interaction in the Gulf Stream at 68°W. Part I: Eddy energetics. *J. Phys. Oceanogr.,* **26,** 2107–2131.

——, E. Carter, and D. R. Watts, 1992: Prediction of the Gulf Stream path from upstream parameters. *J. Geophys. Res.,* **97,** 7257–7269.

Dewar, W. K., and J. M. Bane, 1985: Subsurface energetics of the Gulf Stream near the Charleston Bump. *J. Phys. Oceanogr.,* **15,** 1771–1789.

——, and ——, 1989a: Gulf Stream dynamics. Part I: Mean flow dynamics at 73°W. *J. Phys. Oceanogr.,* **19,** 1558–1573.

——, and ——, 1989b: Gulf Stream dynamics. Part II: Eddy energetics at 73°W. *J. Phys. Oceanogr.,* **19,** 1574–1587.

Glenn, S. M., and C. C. Ebbesmeyer, 1994a: Observations of Gulf Stream frontal eddies in the vicinity of Cape Hatteras. *J. Geophys. Res.,* **99,** 5047–5055.

——, and ——, 1994b: The structure and propagation of a Gulf Stream frontal eddy along the North Carolina shelf break. *J. Geophys. Res.,* **99,** 5029–5046.

Grothues, T. M., and R. K. Cowen, 1999: Larval fish assemblages and water mass history in a major faunal transition zone. *Cont. Shelf Res.,* **19,** 1171–1198.

Hall, M. M., 1994: Synthesizing the Gulf Stream thermal structure from XBT data. *J. Phys. Oceanogr.,* **24,** 2278–2287.

Hogg, N. G., 1986: On the correction of temperature and velocity time series for mooring motions. *J. Atmos. Oceanic Technol.,* **3,** 204–214.

——, 1991: Mooring motion corrections revisited. *J. Atmos. Oceanic Technol.,* **8,** 289–295.

Hood, C. A., and J. M. Bane, 1983: Subsurface energetics of the Gulf Stream cyclonic frontal zone off Onslow Bay, North Carolina. *J. Geophys. Res.,* **88,** 4651–4662.

Howden, S. D., 2000: The three-dimensional secondary circulation in developing Gulf Stream meanders. *J. Phys. Oceanogr.,* **30,** 888–915.

——, and D. R. Watts, 1999: Jet streaks in the Gulf Stream. *J. Phys. Oceanogr.,* **29,** 1910–1924.

Johns, W. E., 1988: One-dimensional baroclinically unstable waves on the Gulf Stream potential vorticity gradient near Cape Hatteras. *Dyn. Atmos. Oceans,* **11,** 323–350.

——, and D. R. Watts, 1986: Time scales and structure of topographic Rossby waves and meanders in the deep Gulf Stream. *J. Mar. Res.,* **44,** 267–290.

Lee, T., and P. Cornillon, 1996a: Propagation and growth of Gulf Stream meanders between 75° and 45°W. *J. Phys. Oceanogr.,* **26,** 225–241.

——, and ——, 1996b: Propagation of Gulf Stream meanders between 74° and 70°W. *J. Phys. Oceanogr.,* **26,** 205–224.

Lee, T. N., J. A. Yoder, and L. P. Atkinson, 1991: Gulf Stream frontal eddy influence on productivity of the southeast U.S. continental shelf. *J. Geophys. Res.,* **96,** 22 191–22 205.

Lindstrom, S., and D. R. Watts, 1994: Vertical motion in the Gulf Stream near 68°W. *J. Phys. Oceanogr.,* **24,** 2321–2333.

——, X. Qian, and D. R. Watts, 1997: Vertical motion in the Gulf Stream and its relation to meanders. *J. Geophys. Res.,* **102,** 8485–8503.

Luther, M., and J. M. Bane, 1985: Mixed instabilities in the Gulf Stream over the continental slope. *J. Phys. Oceanogr.,* **15,** 3–23.

Miller, J. L., 1994: Fluctuations of Gulf Stream frontal position between Cape Hatteras and the Straits of Florida. *J. Geophys. Res.,* **99,** 5057–5064.

——, and T. N. Lee, 1995: Gulf Stream meanders in the South Atlantic Bight: 1. Scaling and energetics. *J. Geophys. Res.,* **100,** 6687–6704.

Pedlosky, J., 1987: *Geophysical Fluid Dynamics.* 2d ed. Springer-Verlag, 710 pp.

Percival, D. B., and A. T. Walden, 1993: *Spectral Analysis for Physical Applications: Multitaper and Conventional Univariate Techniques.* Cambridge University Press, 583 pp.

Pickart, R. S., 1994: Interaction of the Gulf Stream and deep western boundary current where they cross. *J. Geophys. Res.,* **99,** 25 155–25 164.

——, 1995: Gulf Stream–generated topographic Rossby waves. *J. Phys. Oceanogr.,* **25,** 574–586.

——, and D. R. Watts, 1990: Deep western boundary current variability at Cape Hatteras. *J. Mar. Res.,* **48,** 765–791.

——, and W. M. Smethie, 1993: How does the deep western boundary current cross the Gulf Stream? *J. Phys. Oceanogr.,* **23,** 2602–2616.

Pond, S., and G. L. Pickard, 1983: *Introductory Dynamical Oceanography.* 2d ed. Pergamon Press, 329 pp.

Rossby, T., 1987: On the energetics of the Gulf Stream at 73W. *J. Mar. Res.,* **45,** 59–82.

Savidge, D. K., 2002: Wintertime shoreward near-surface currents south of Cape Hatteras. *J. Geophys. Res.,* **107,** 3205, doi: 10.1029/2001JC001193.

——, and J. M. Bane, 1999a: Cyclogenesis in the deep ocean beneath the Gulf Stream. 1. Description. *J. Geophys. Res.,* **104,** 18 127–18 140.

——, and ——, 1999b: Cyclogenesis in the deep ocean beneath the Gulf Stream. 2. Dynamics. *J. Geophys. Res.,* **104,** 18 111–18 126.

——, and ——, 2001: Wind and Gulf Stream influences on along-shelf transport and off-shelf export at Cape Hatteras, North Carolina. *J. Geophys. Res.,* **106,** 11 505–11 527.

——, T. J. Shay, and J. M. Bane, 1993: Synoptic Ocean Prediction Experiment: EN216 CTD section data report. Tech. Rep. CMS93-1, University of North Carolina, Chapel Hill, NC, 15 pp.

Spall, M. A., 1996a: Dynamics of the Gulf Stream/deep western boundary current crossover. Part I: Entrainment and recirculation. *J. Phys. Oceanogr.,* **26,** 2152–2168.

——, 1996b: Dynamics of the Gulf Stream/deep western boundary current crossover. Part II: Low-frequency internal oscillations. *J. Phys. Oceanogr.,* **26,** 2169–2182.

Sutyrin, G. G., I. Ginis, and S. A. Frolov, 2001: Equilibration of baroclinic meanders and deep eddies in a Gulf Stream–type jet over a sloping bottom. *J. Phys. Oceanogr.,* **31,** 2049–2065.

Tansley, C. E., and D. P. Marshall, 2000: On the influence of bottom topography and the deep western boundary current on Gulf Stream separation. *J. Mar. Res.,* **58,** 297–325.

Tracey, K. L., and D. R. Watts, 1986: On Gulf Stream meander characteristics near Cape Hatteras. *J. Geophys. Res.,* **91,** 7587–7602.

Vazquez, J., and D. R. Watts, 1985: Observations on the propagation, growth, and predictability of Gulf Stream meanders. *J. Geophys. Res.,* **90,** 7143–7151.

Verity, P. G., J. Bauer, C. N. Flagg, D. DeMaster, and D. Repeta, 2002a: The ocean margins program: An interdisciplinary study of carbon sources, transformations, and sinks in a temperate continental margin system. *Deep-Sea Res.,* **49B,** 4273–4295.

——, D. G. Redalje, S. R. Lohrenz, C. Flagg, and R. Hristov, 2002b: Coupling between primary production and pelagic consumption in temperate ocean margin pelagic ecosystems. *Deep-Sea Res.,* **49B,** 4553–4569.

Watts, D. R., and W. Johns, 1982: Gulf Stream meanders: Observations on propagation and growth. *J. Geophys. Res.,* **87,** 9467–9476.

——, K. L. Tracey, J. M. Bane, and T. J. Shay, 1995: Gulf Stream path and thermocline structure near 74°W and 68°W. *J. Geophys. Res.,* **100,** 18 291–18 312.

Webster, F. A., 1961: A description of Gulf Stream meanders off Onslow Bay. *Deep-Sea Res.,* **8,** 130–143.